Open Access

ORIGINAL ARTICLE

Prostate Disease

Prenatal and pubertal testosterone exposure imprint permanent modifications in the prostate that predispose to the development of lesions in old Mongolian gerbils

Manoel F Biancardi[1,2], Ana PS Perez[1], Cássia RS Caires[3], Luiz R Falleiros Jr[3], Rejane M Góes[3],
Patrícia SL Vilamaior[3], Diógenes R Freitas Jr[4], Fernanda CA Santos[2], Sebastião R Taboga[1,3]

The prostate is an accessory sex gland that develops under precise androgenic control. It is known that hormonal imbalance may disrupt its development predisposing this gland to develop diseases during aging. Although the hypothesis regarding earlier origins of prostate diseases was proposed many years ago, the mechanisms underlying this complex phenomenon are poorly understood. Therefore, the aim of this study was to evaluate the prostates of old male gerbils exposed to testosterone during intrauterine and postnatal life using morphological, biometrical, stereological, Kariometric, immunohistochemical, and immunofluorescence analyses. Our findings demonstrate that prenatal and pubertal exposure to testosterone increases the susceptibility to the development of prostate diseases during aging. The presence of a more proliferative gland associated with foci of adenomatous hyperplasia in animals exposed to testosterone during the prenatal and pubertal phase show that the utero life and the pubertal period are important phases for prostatic morphophysiology establishment, which is a determinant for the health of the gland during aging. Therefore, these findings reinforce the idea that prostate disease may result from hormonal disruptions in early events during prostate development, which imprint permanently on the gland predisposing it to develop lesions in later stages of life.

INTRODUCTION

Studies have been emphasizing that prostatic diseases such as benign prostatic hyperplasia (BPH) and prostate cancer originate from direct influences during uterine life,[1] with androgenic imbalance as one of the most critical causes.[2] Although the mechanisms underlying the early origin of prostatic diseases are still poorly understood, hormonal influences are one of the most critical causes for these diseases.[3]

There are several factors which may be responsible for disrupting critical moments of the prenatal period of prostate development such as hyperandrogenism, polycystic ovary syndrome (PCOS)[4] dietary, and steroid intake, besides exposure to endocrine-disrupting chemicals (EDCs).[5] Although most literature reports have emphasized the influence of EDCs with estrogenic potential,[5–7] some studies have shown the impact of disruption, by androgenic compounds, on prostate development in male and female rodents.[8–11]

A recent study by our research group showed that abnormal testosterone exposure during prenatal life may be directly related to the development of premalignant prostate diseases during adult life

in the Mongolian gerbil.[11] However, there is a lack of studies on the impact of androgenic imbalance during early moments of life and the consequences on the prostate gland of old individuals.

Thus, considering that prostate development is an event that depends on fine hormonal control,[12] sensible interferences may imbalance programs of gene expression leading to irreversible changes in prostate morphogenesis and maintenance during aging. Therefore, an understanding of events that may interfere with prostate organogenesis may help elucidate the mechanisms underlying the origin of prostate diseases.

Recent evidence has demonstrated that exposure to estradiol and bisphenol-A (BPA) during prostate development is directly linked to an epigenetic alteration of this gland, increasing the susceptibility to prostate carcinogenesis with aging.[5] This evidence is very important to gain insight into the early events of prostate development and its relation with the origin of prostate diseases.

Considering all these aspects, our hypothesis is that abnormal prenatal exposure to testosterone may disrupt the normal process of

[1]Department of Structural and Functional, State University of Campinas, Av. Bertrand Russel s/n, Campinas, São Paulo, 13084864, Brazil; [3]University Estadual Paulista – UNESP, Department of Biology, Laboratory of Microscopy and Microanalysis, Rua Cristóvão Colombo, 2265, São José do Rio Preto, São Paulo, 15054000, Brazil; [4]Medical School, Federal University of Goiás, Colemar Natal e Silva, Goiânia, Goiás, 74001970, Brazil; [2]Department of Histology, Embryology and Cell Biology, Federal University of Goiás, Samambaia II, Goiânia, Goiás, 74001970, Brazil.
Correspondence: Dr. SR Taboga (taboga@ibilce.unesp.br)
Received: 24 March 2015; Revised: 24 June 2015; Accepted: 30 October 2015

prostate development increasing the susceptibility to the development of prostatic diseases during aging. Thus, the aim of this study was to evaluate the prostate of old gerbils that were exposed to testosterone during prenatal and pubertal life.

MATERIALS AND METHODS

Animals and experimental design

The animals were provided by the São Paulo State University (UNESP) (São José do Rio Preto) and maintained in polyethylene cages under controlled conditions of light and temperature, provided with filtered water and rodent food *ad libitum*. Animal handling and experiments were performed according to the ethical guidelines of the São Paulo State University (UNESP) (Ethical Committee number 021/09 CEUA), following the Guide for Care and Use of Laboratory Animals. During all experiments, we provided filtered water in glass bottles to avoid the release of endocrine-disrupting chemicals such as bisphenol-A from plastic material.

We used 20 adult females and 20 adult males (between 3 and 4 months old) of gerbils (*Meriones unguiculatus*, Muridae: gerbillinae) for mating. We matched, randomly, one male and one female to form independent families. Five couples were put into each group. Pregnant females from these couples underwent different manipulations, and their male offspring formed all experimental groups, as follows: C (control) group: male offspring from nonmanipulated pregnant females; male C + T (testosterone during puberty) group: male offspring from nonmanipulated pregnant females. The littermate was treated with subcutaneous injections of 100 µg of T (testosterone cypionate – deposteron; EMS) diluted in 100 µl of mineral oil during the 6th, 7th, and 8th weeks of life; TG (testosterone during gestation) group: male offspring from mothers exposed to subcutaneous injections of 500 µg of T during gestation. TG + T (testosterone during gestation plus puberty) group: male offspring from mothers exposed to subcutaneous injections of 500 µg of T during gestation plus subcutaneous injections of 100 µg of T during the 6th, 7th, and 8th weeks of life. Only the pups exposed to testosterone that were born 4 days after treatment were employed in this study. The litters employed in this study were obtained at least from three different couples for each analyzed group. All animals utilized in this study were killed after 1 year of birth. The protocol of T treatment was adapted from Wolf and coworkers.[8] The overall experimental design, treatment details with T and the age at which the animals were killed are shown in **Figure 1**.

All animals were killed by CO_2 inhalation followed by decapitation. We collected blood samples. Body, prostatic complex (PrC - correspondent urethral segment, ventral, dorsolateral and dorsal prostate lobes), testis, and adrenals were weighed. These fragments were dissected out using a Leica stereoscopic microscope (Leica, Germany) to remove adipose tissues and isolate the urethral segment plus the associated prostatic tissue. The anogenital distance (AGD) measurements were obtained with a digital caliper rule.

Light microscopy

The PrCs from male gerbils were fixed by immersion in 4% paraformaldehyde (buffered in 0.1 mol l^{-1} phosphate, pH 7.2) or in metacarn (proportions: methanol 60%, chloroform 30% and acetic acid 10%) for 3 h. After fixation, the tissues were washed in water, dehydrated in ethanol, clarified in xylene and embedded in paraffin (Histosec, Merck, Dermstadt, Germany). Serial tissue sections of 5 µm were obtained for all tissue fragments using an automatic rotator microtome (Leica RM2155, Nussloch, Germany). The sections were stained with hematoxylin-eosin (H and E) and picrosirius for general morphological analysis. Prostatic reticular fibers and elastic fibers were identified, respectively, by Gömöri's reticulin and resorcin-fuchsin techniques. The specimens were analyzed with an Olympus BX60 light microscope (Olympus, Tokyo, Japan), and the images were digitalized using the software DP-BSW V3.1 (Olympus).

Stereological and kariometric analysis

The stereological analyses were carried out using Weibel's multipurpose graticule with 130 points and 10 test lines[13] to compare the relative proportion (relative volume) of each component of the prostatic tissue (epithelium, lumen and muscle and nonmuscle stroma), as described by Huttunen and coworkers.[14] We chose thirty microscopic fields at random from each experimental group (6 fields/animal; $n = 5$). In summary, we determined the relative values by counting the coincident points in the test grid and dividing them by the total number of points.

Nuclear area, perimeter and form factor data were obtained from 50 microscopic fields (subjected to Feulgen reaction) randomly taken from each experimental group (10 fields/animal; $n = 5$). Form factor is used as a measure to check the roundness status of the cell nuclei, being that nuclear form factor close to 1 index indicates that the cell nucleus is more round and less elliptic. From these 50 microscopic fields, we randomly obtained the area and perimeter data from 400 nuclei for each group ($n = 5$ animals/group). Indeed, we obtained
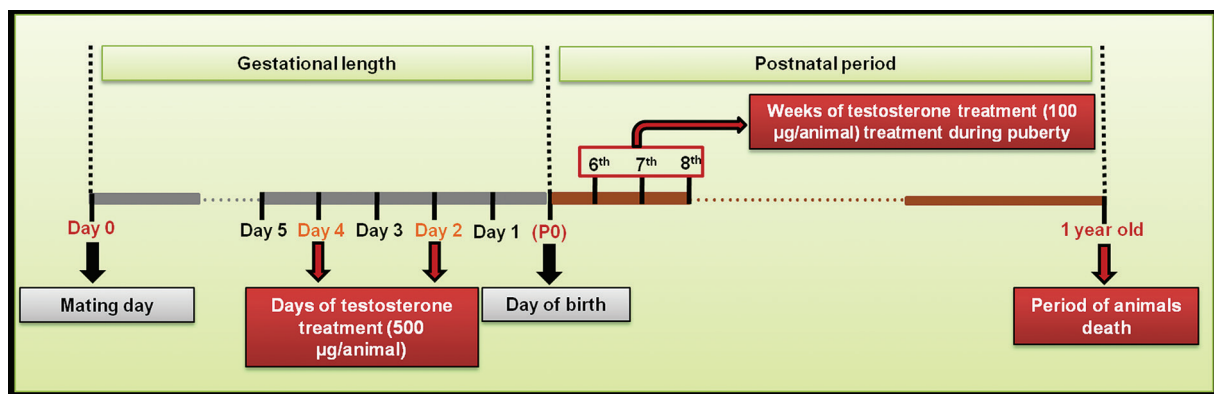

Figure 1: Schematic representation of the experimental protocol employed in this study. The interval between day 0 (day of mating) and day P0 (day of birth) represents the gerbil gestational period. The days 4 and 2 represent the prenatal days of testosterone treatment (groups TG and TG + T). The 6th, 7th, and 8th represent the pubertal weeks in which the animals were weekly treated with testosterone (groups CT and TG + T). The end of the timeline (1-year-old) represents the age of the animals' death.

form factor data employing (4π × nuclear area/[nuclear perimeter]^2). Stereological and kariometric analyses were taken using the software Image-Pro Plus version 6.1 for Windows (Media Cybernetics Inc., Silver Spring, MD, USA).

Immunohistochemistry

Tissue sections were subjected to immunohistochemistry for the detection of the androgen receptor (AR), estrogen receptor-alpha (ER-α), and proliferating cell nuclear antigen (PCNA). Primary antibodies reactive to AR (rabbit polyclonal IgG, N-20, Santa Cruz Biotechnology, CA, USA), ER-α (rabbit polyclonal IgG, MC-20, Santa Cruz Biotechnology), p63 (mouse monoclonal IgG$_{2a}$, sc-843, 4A4, Santa Cruz Biotechnology, CA, USA) and PCNA (mouse monoclonal IgG$_{2a}$, SC 56, Santa Cruz Biotechnology, CA, USA) were employed at a dilution of 1:100. Peroxidase-conjugated specific antibodies (Sigma Chemical Co., Saint Louis, MO, USA) or polymers (Post Primary Block and polymer, Novocastra, Newcastle Upon Tyne, UK; DAKO Envision™ + Dual link system-HRP, K4061) were used as secondary antibodies and incubated with samples for 45 min at 37°C. The sections were reacted with diaminobenzidine and counterstained with Harris's hematoxylin. The histological sections were analyzed with a Olympus BX60 light microscope (Olympus, Tokyo, Japan).

AR and PCNA quantification

For AR quantification, 30 microscopy fields (magnification of 400×) were used for each experimental group. From each animal, we used 10 fields, being a total of three animals (from different litters) for each experimental group. In each field, the total number of positive epithelial and stromal cells was obtained as a relative frequency (%) in relation to the total number of negative epithelial or stromal cells. Between positive and negative cells, we counted a mean of 5300 epithelial cells and 1300 stromal cells for each experimental group.

Regarding PCNA quantification, we employed 50 microscopy fields (magnification of 400×) for each experimental group. As aforementioned, from each animal we used 10 fields, being a total of three animals (from different litters) for each experimental group in each field, the total number of positive epithelial cells was obtained as a relative frequency (%) in relation to the total number of epithelial cells of the acini. Between positive and negative cells, we counted a mean of 6000 epithelial cells for each experimental group. All these analyses were performed using the image analysis system previously described.

Immunofluorescence

Tissue sections were subjected to immunofluorescence for the detection of smooth muscle α-actin (mouse monoclonal IgG$_{2a}$, sc-32251, IA4, Santa Cruz Biotechnology, CA, USA), which was incubated at a dilution of 1:100 overnight. The next morning, the sections were incubated with fluorochrome-conjugated specific secondary antibodies (anti-mouse, sc-2010, IgG-FITC, Santa Cruz Biotechnology, CA, USA) for 2 h at room temperature. DAPI was employed to identify the cell nuclei. The histological sections were analyzed with a Zeiss Imager M2 fluorescence microscope (Zeiss, Göttingen, Germany) coupled to the AxioVision (Zeiss, Germany) software and laser-scanning microscope (LSM 710; Zeiss, Jena, Germany).

Statistical analyses

The hypothesis tests employed to determine statistical significance were the Kruskal–Wallis test for nonparametric distributions and ANOVA for parametric distributions. Further determination of the significant statistical differences between experimental groups was done using Dunn's test for nonparametric distributions and Tukey's test for parametric distributions. For kariometric data, mean values were calculated for each animal inside each experimental group, and the resulting 5 data points per dose group were compared with the appropriate statistical test as mentioned above. The data were analyzed using Statistica 6.0 (StarSoft, Inc., Tulsa, OK, USA) and BioEstat 5.0 (http://mamiraua.org.br/pt-br/downloads/programas/) software (Copyrigth 2015, Instituto de Desenvolvimento Sustentavel Mamirauá, Tefé, AM, Brazil). The level of significance was set at 5% ($P \leq 0.05$). Values are presented as mean ± standard error of the mean.

RESULTS

Biometrical, stereological, and kariometric analysis

Regarding the biometrical analyses, we did not observe statistically significant differences between the variables of experimental groups. Stereological analyses of prostate compartments demonstrated statistically significant differences only for muscle relative volume between the C + T and TG groups. Regarding kariometric analysis, we did not observe any significant difference for the variables nuclear area and nuclear perimeter between the experimental groups. However, nuclear form factor data were significantly increased in all treated groups (**Table 1**).

Morphological aspects of the ventral prostate

Through morphological characterization (**Figure 2a–2p**) of H and E-stained sections, we observed the presence of hyperplasic lesions in all experimental groups. However, lesions characterized by adenomatous hyperplasia were found only in the prostate of the TG + T group (**Figure 2m** and **2o**).

Stromal analyses employing Gömöri's reticulin, picrossirius and resorcin-fuchsin techniques (**Figure 3a–3n**) showed an intense stromal reshuffling that affected regions with lesions, especially in the prostates of the TG and TG + T groups. Regarding the collagen fibers, we identified foci with intense collagen remodeling in injured regions (**Figure 3c, 3e, 3i, 3j**) of these groups. In addition, in the TG + T group, we observed a severe collagen alteration surrounding regions affected by adenomatous hyperplasia, where the fibers presented a fragmented disposing (**Figure 3j**).

Table 1: Biometrical, stereological, and kariometric data of the experimental groups

Variables	Groups			
	C	C + T	TG	TG + T
Biometrical analysis				
Body weight (g)	82.7±3.4	84.4±5.7	80.7±4.4	77±2.0
PrC weight (g)	0.96±0.09	1.03±0.04	0.99±0.79	1.01±0.03
Testis weight (g)	1.19±0.04	1.17±0.05	1.17±0.03	1.19±0.03
Adrenal weight (g)	0.044±0.003	0.046±0.002	0.048±0.002	0.045±0.003
AGD (mm)	16.03±0.39	15.37±0.41	16.24±0.29	15.30±0.20
Stereological analysis (%)				
Epithelium	23.26±1.84	21.77±2.38	27.05±2.58	25.95±1.88
Lumen	45.54±3.01	47.72±3.84	42.31±3.63	42.02±3.37
Muscle stroma	9.13±0.69^{a,b}	7.26±0.81^b	10.31±0.85^a	8.48±0.77^{a,b}
Nonmuscle stroma	22.08±2.14	23.26±2.31	20.33±1.79	23.54±2.05
Kariometric analysis				
Nuclear area (μm^2)	31.96±0.44	32.29±0.57	32.71±0.80	33.24±0.39
Nuclear perimeter (μm)	22.08±0.15	22.18±0.17	21.76±0.24	21.83±0.09
Nuclear form factor	0.82±0.01^a	0.88±0.01^b	0.87±0.01^b	0.88±0.01^b

Values are expressed as mean±s.e.m. (*n*=6 animals/group; for kariometrical analysis we employed 5 animals/group). Superscript letters (a and b) represent statistically significant (*P*≤0.05) differences between the experimental groups. Experimental groups with values that have the same letters did not show statistically significant differences. s.e.m.: standard error of the mean; PrC: prostatic complex; AGD: anogenital distance
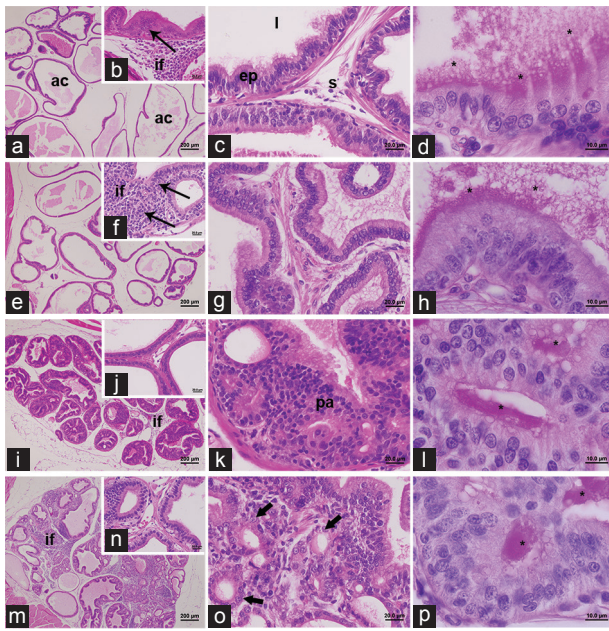
Figure 2: Morphological characterization of prostates by H and E and PAS techniques. (**a–h**) show morphological aspects of the C (**a–d**), C + T (**e–h**), TG (**i–l**), and TG + T (**m–p**) prostates. Although we observed some prostatic lesions in the C, C + T and TG groups (**b, f, k**), the TG + T group showed a more severely injured gland, affected mainly by adenomatous hyperplasia associated with inflammatory foci (**m** and **o**). Note the presence of inflammatory foci in prostates of all groups (**b, f, i, m**). The pattern of secretion showed a similar pattern in all experimental groups (**d, h, l, p**). ac: acini; ep: epithelium; l: lumen; s: stroma; if: inflammatory foci; arrows: prostatic lesions; large arrows: adenomatous hyperplasia; asterisk: glycoprotein secretion stained by PAS; pa: proliferative area. Scale bar: 200 μm in **a, e, i, m**; 20 μm in **b, c, f, g, j, k, n, o**; 10 μm in **d, h, l, p**.

Regarding the elastic system, the C and C + T groups presented prostates with elastic fibers normally disposed around the acini (**Figure 3k** and **3l**), except in some cases of prostatic lesions, in which we observed a significantly altered pattern of elastic components. For the groups TG and TG + T, these fibers were dispersed and almost absent in regions with lesions (**Figure 3m** and **n**).

Immunohistochemical aspects of the male ventral prostate

Androgen receptor (AR) immunolocalization showed a similar pattern in all experimental groups in both epithelial and stromal compartments (**Figure 4a–4d**). However, the AR quantification showed a significant increase in the number of AR-positive cells in both epithelial ($P \leq 0.05$) and stromal compartments ($P \leq 0.01$) of the C + T group in comparison with the C and TG + T groups (**Figure 5a** and **b**). Quantitative analysis has also shown an increase of AR-positive cells in the stromal compartment in the TG group in comparison with the C and TG + T groups ($P \leq 0.01$; **Figure 5b**).

Using immunohistochemistry for PCNA, we observed a statistically significant increase of the proliferative cells in the prostates of the TG + T (**Figure 4h**) group in comparison with the C, C + T and TG groups (**Figure 4e–4g**). This was confirmed by the quantification of the PCNA-positive cells distributed in the epithelial compartment of the gland (**Figure 5c**).

Regarding ERα, we observed a similar pattern of immunolocalization in the C and C + T prostates (**Figure 6a** and **6b**), in which we noted a rare presence of this receptor only in the stromal compartment. On the other hand, in the prostate of TG and TG + T, in addition to
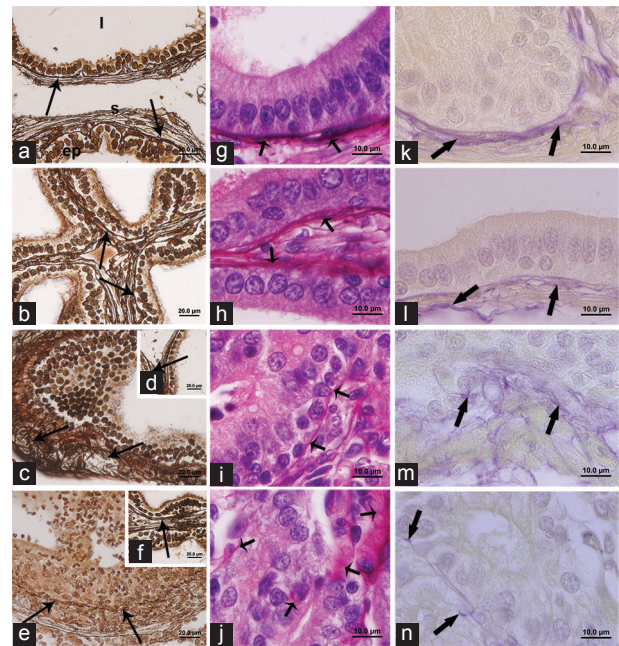

Figure 3: Gömöri's reticulin, picrossirius, and resorcin-fucsin techniques for identification of reticular fibers (collagen III), general collagen, and elastic fibers. (**a–n**) show morphological aspects of the C (**a, g, k**), C + T (**b, h, l**), TG (**c, d, l, m**), and TG + T (**e, f, j, n**) prostates. (**a** and **b**) The regular localization of reticular fibers adjacent to the prostatic epithelium in the C and C + T groups. (**c** and **e**) On the other hand, the groups TG and TG + T showed some areas with reshuffling of these fibers, mainly in regions affected by lesions. (**d** and **f**) Inserts show the disposing of collagen III in unaffected TG and TG + T prostates. (**i** and **j**) Regarding general collagen, the prostates of TG and TG + T presented a high reshuffling of these fibers, specifically in injured regions. (**m** and **n**) Regarding the elastic system, we observed several regions with a changed pattern of these stromal components in both TG and TG + T. (**n**) Regions affected by adenomatous hyperplasia showed a reduced quantity of elastic fibers. ep: epithelium; l: lumen; s: stroma; arrows: reticular fibers; short arrows: general collagen; large arrows: elastic fibers. Scale bar: 20 μm in **a–f**; 10 μm in **g–n**.

stromal immunolocalization, we also detected a marking of ERα in the epithelial compartment of the acini (**Figure 6c** and **6d**).

P63 protein showed a similar pattern of immunolocalization in the prostate of the C, C + T, and TG groups (**Figure 6e–g**), being characterized by the presence of basal cells in the basal acinar layer. However, we observed an abnormal immunolocalization of p63-positive cells in some foci of TG and TG + T prostates (**Figure 6g** and **6h**). Indeed, in some regions of TG + T prostates, we did not detect the presence of p63-positive basal cells (**Figure 6h**).

Immunofluorescence analysis of smooth muscle α-actin

Immunofluorescence analysis of smooth muscle α-actin has shown a high heterogeneity of this stromal element in the prostates of the experimental groups. In the C and C + T prostates, we detected a normally smooth muscle distributed around the gland acini (**Figure 7a–7d**). However, in the TG and TG + T prostates this stromal element was absent in some areas, especially around regions with lesions (**Figure 7e–7h**). Furthermore, in some cases relating TG + T prostates, we did not detect the presence of a smooth muscle layer in adjacent regions affected by adenomatous hyperplasia (**Figure 7g** and **7 h**).

DISCUSSION

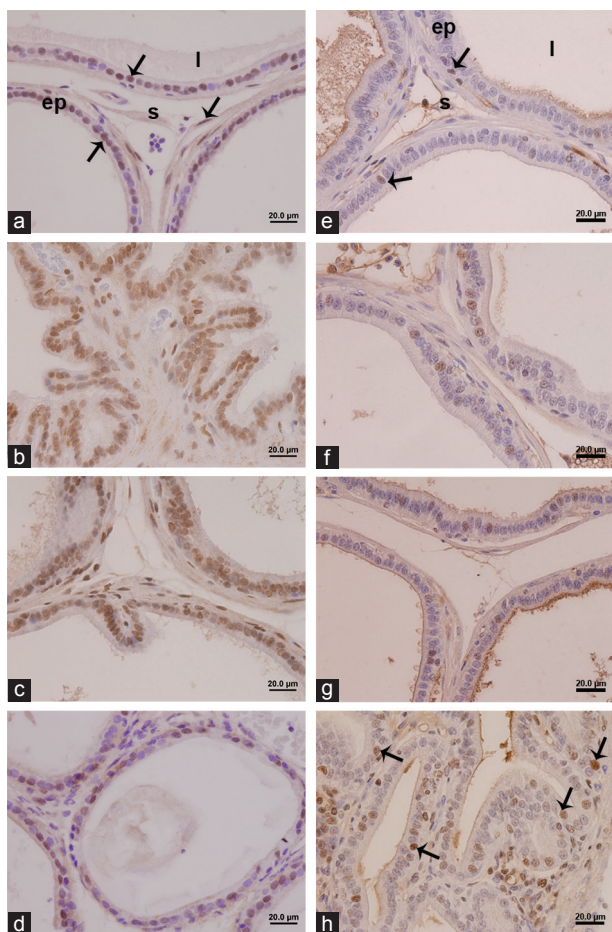This study showed that old male gerbils exposed to testosterone during

Figure 4: Immunohistochemistry for AR and PCNA. (**a–d**) AR immunolocalization in both epithelial and stromal compartments of the prostate in all experimental groups. **e–h** demonstrate the immunolocalization of PCNA in the prostates. Observe the high number of PCNA-positive cells in the prostates of the TG + T group (**h**). ep: epithelium; l: lumen; s: stroma; arrows: positive cells to AR and PCNA. (**a** and **e**) C, (**b** and **f**) C + T, (**c** and **g**) TG and (**d** and **h**) TG + T. Scale bar: 20 μm in **a–h**.

Figure 5: Graphical representation of AR and PCNA quantification. Observe the significant increase of AR-positive cells in both epithelial (**a**) and stromal (**b**) compartments of C + T prostates in comparison with the C group. AR-positive stromal cells have also increased in the prostates of the TG group in comparison with the C group (**b**). Regarding PCNA quantification, the TG + T group showed a significant increase of PCNA-positive cells in comparison with the C, C + T and TG groups (**c**). Asterisks indicate statistically significant differences between experimental groups (*$P \leq 0.05$; **$P \leq 0.01$).

prenatal and pubertal phases (TG + T group) had a higher propensity to develop prostatic lesions during aging. Although we detected hyperplastic foci in the prostates of all experimental groups, lesions such as adenomatous hyperplasia associated with inflammatory foci were observed only in prostates of the TG + T group. Indeed, we observed an increase in the proliferative rate in the glands of the TG + T group, as determined by PCNA counting. These findings suggest that the association of both periods of treatment (prenatal and pubertal) are necessary to increase the susceptibility of the gland to developing lesions with aging.

Regarding morphological analyses, the prostates of all experimental groups have presented, somehow, lesions with hyperplastic foci. We found both epithelial and stromal compartments changed in regions containing lesions either in control or treated groups. The presence of spontaneous prostatic lesions in old gerbils has been well characterized by researchers of our group in previous studies.[15] These results showed that gerbils, in contrast to other rodents such as rats and mice, have a biological condition to develop prostatic lesions during aging. This congenital condition of male gerbils to develop prostatic lesions is still poorly understood, lacking of a definitive reference available in the literature.

The most differential morphological aspect observed was the presence of adenomatous hyperplasia in the prostates of TG + T
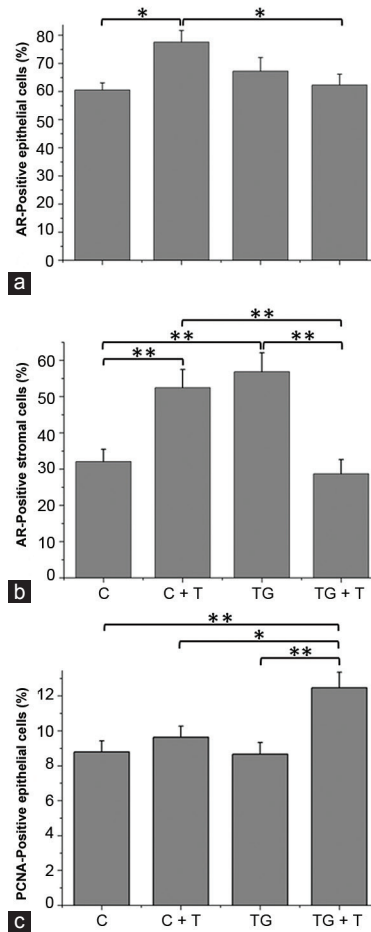
animals. This pathological condition is characterized by the proliferation of small acini from the normal acini, which is easily mistaken with prostatic adenocarcinoma.[16–18] Although the precursor nature of adenomatous hyperplasia remains uncertain, some recent evidence supports that adenomatous hyperplasia may be a precursor lesion of prostate cancer.[18]

Although the data of biometrical and stereological analyses have not presented any significant aspect between the experimental groups, the kariometric data showed some differences for the nuclear form factor. We did not find any statistically significant difference regarding nuclear area and nuclear perimeter between treated groups (C + T, TG, TG + T) in comparison with the C group. On the other hand, we observed an increase of the nuclear form factor index in all treated groups in comparison with the C group.

The form factor has been used as a measure to check the roundness status of the cell nucleus. Nuclear form factor values close to 1 index indicate that the cell nucleus is more round and less elliptic.[19] Some studies have employed this parameter in cases of BPH and prostate adenocarcinoma,[20] or in studies showing the synthesizing status of the prostatic cells when subjected to testosterone supplementation.[19] Here,
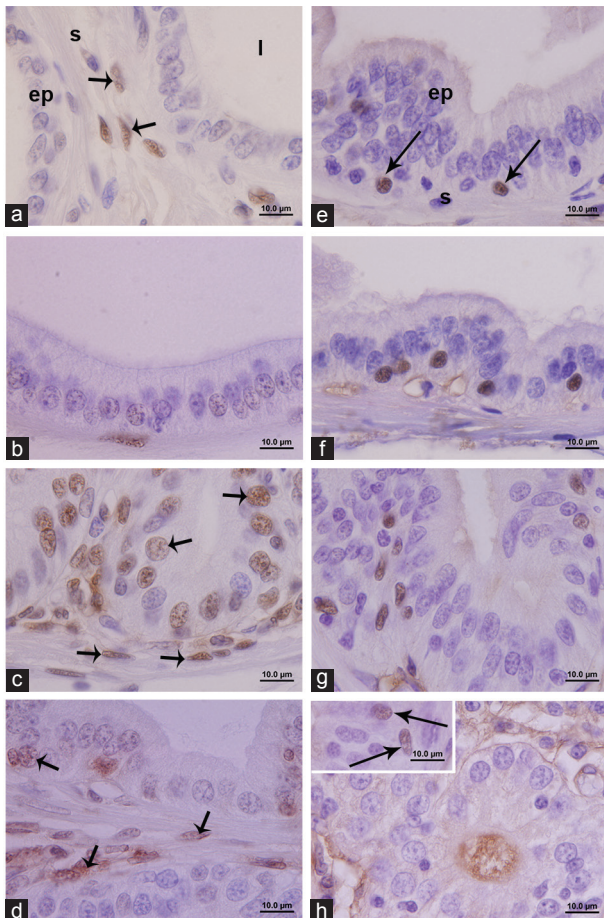
Figure 6: Immunohistochemistry for ERα and p63 proteins. (**a–d**) The stromal expression of ERα for all experimental groups. Observe the expression of ERα in the epithelium of TG and TG + T prostates (**c** and **d**), which suggests a more proliferative status between these experimental groups. **e–h** demonstrate the immunolocalization of p63 protein in the basal cell population in the prostate epithelium. We observed that the regularity of this cellular layer is lost in some injured areas of the prostate in the TG and TG + T groups (**g** and **h**), suggesting a changed pattern of p63 immunolocalization. Observe the absence of basal cells in some regions of the adenomatous hyperplasia (**h**). ep: epithelium; l: lumen; s: stroma; small arrows: ERα-positive cells; arrows: p63-positive cells. (**a** and **e**) C, (**b** and **f**) C + T, (**c** and **g**) TG and (**d, h, i**) TG + T. Scale bar: 20 μm in **a–h**.

Figure 7: Immunofluorescence for smooth muscle α-actin. (**a–d**) The normal pattern of smooth muscle surrounding the epithelium in the prostates of the C and C + T groups. (**e–h**) Observe the absence of the smooth muscle layer (SML) in the prostates of TG and TG + T injured by lesions. ac: acini; ep: epithelium; l: lumen; s: stroma; arrows: smooth muscle layer; large arrows: regions lacking smooth muscle; Scale bar: 200 μm in **a, c, e, g**; Scale bar: 20 μm in **b, d, f, h**. (**a** and **b**) C, (**c** and **d**) C + T, (**e** and **f**) TG and (**g** and **h**) TG + T.

we observed an increase of the circular shape in the nuclei of epithelial prostatic cells of all treated groups, showing that this parameter was, somehow, affected by the treatments.

Regarding immunohistochemical analyses for AR, we observed a similar pattern of immunolocalization in both epithelial and stromal cells between the experimental groups. However, employing AR quantification we detected an increase of AR-positive cells in both epithelial and stromal compartments of the prostate in C + T animals, whereas only AR-positive stromal cells showed an increase in the prostates of the TG group in comparison with the C group. Although the glands of C + T animals contained a higher number of AR-positive cells, we did not observe any association of this fact with a possible increase in the proliferative rate in this experimental group or with the development of lesions such as adenomatous hyperplasia. Although we are unable to explain the molecular basis of these differences regarding the increase of AR-positive cells in C + T and TG groups, some events of DNA imprinting may be involved.
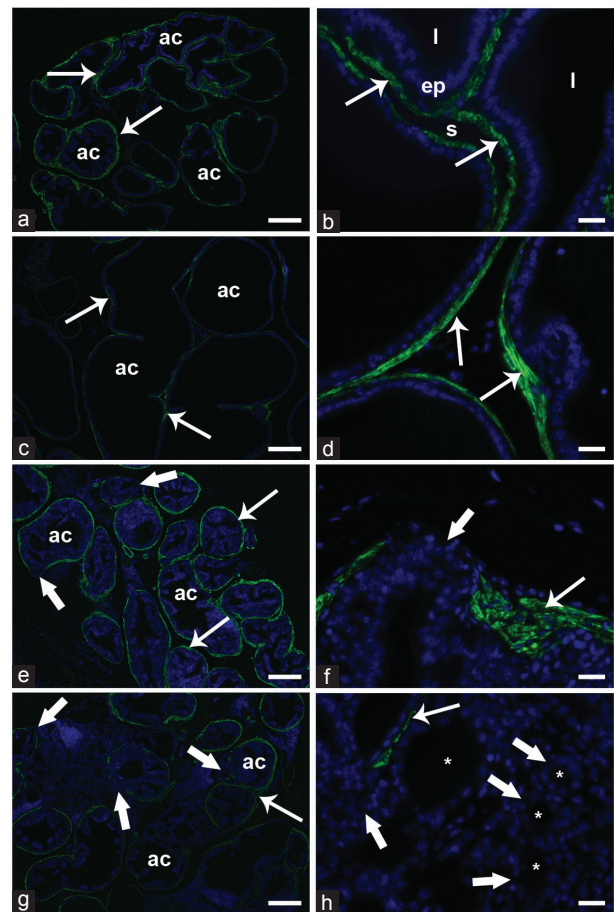
Recent studies have been investigating the influence of endocrine disruptors on the epigenome during early stages of prostate development.[5] According to these authors, exposure to estrogenic compounds (estradiol and BPA) imprint the prostate to an increased susceptibility to the development of carcinogenesis during aging. Prins and collaborators.[5] have shown a changed pattern of DNA methylation in multiple cell signaling genes, which suggested an epigenetic mechanism of action. Because the mechanisms underlying the origin of prostate diseases are unknown, an understanding of the molecular basis of these events responsible to imprint prostates may open new strategies to prostate disease therapy.

Another relevant aspect was the increase of proliferation in the epithelial compartment of TG + T prostates, as determined by PCNA-positive cell counting. The data showed a statistically significant increase in the proliferative rate only in the prostates of the TG + T groups in comparison with other experimental groups. These data are in consistent with the presence of several foci of adenomatous hyperplasia in the glands of these animals, as shown in H and E sections.

Regarding ERα immunolocalization, we observed a different pattern of localization between the groups. Whereas we observed only stromal cells positive to ERα in C and C + T prostates, in TG and

TG + T we detected ERα-positive cells in both stromal and epithelial compartments. Because ERα has been associated with an aberrant proliferative role, which may lead to the development of lesions in the prostate,[21] these findings suggested that the prostates of TG and TG + T were influenced by ERα pathways related to an increase in the proliferative status.

Regarding p63 immunomarking, we observed an altered pattern of p63 immunolocalization in the prostates of TG and TG + T. In these prostates, we detected an alteration of p63 immunolocalization in the basal layer, being possible to localize p63-positive cells out of the basal layer, especially in foci of lesions. This evidence is consistent with literature studies that showed the loss of p63 expression in the basal layer, causing a changed pattern of p63 expression in these cases.[22] Moreover, in some regions affected by adenomatous hyperplasia in the TG + T prostates, we observed a scattered pattern of p63-positive basal cells in some acini. These findings are in consistent with recent findings by Zhang and collaborators[18] who showed a fragmented pattern of the basal layer in regions of the human prostate affected by atypical adenomatous hyperplasia (AAH).

The immunofluorescence analyses for smooth muscle α-actin showed several regions with an interruption or absence of the smooth muscle layer surrounding injured regions in the prostates of TG and TG + T. Furthermore, in TG + T prostates we observed large regions of adenomatous hyperplasia with a complete absence of smooth muscle α-actin, which suggests the presence of new invasive buds in the adjacent stroma.

In addition to the aforementioned results, we also detected the presence of some inflammation foci in the prostate of all experimental groups, in particular associated with the lesions of the TG + T group. However, it is unclear to us if this inflammatory state may have occurred due to a primary effect of the treatment or if it occurred secondarily due to the presence of lesions in the prostate. These questions need to be further explored in future studies since some reports have proposed a new hypothesis for prostate carcinogenesis, which changes the view regarding the origin of prostate cancer. A recent review by De Marzo and collaborators showed some important aspects of the relation between inflammation and prostate carcinogenesis.[23] According to these authors, there are several potential sources for the inflammation, such as direct infection, reflux urine, inducing chemical and physical trauma, dietary factors, estrogens, or a combination of these. Any of these factors has the potential to break the immune tolerance leading to an autoimmune reaction in the prostate.[23]

Recent researches have given special attention to questions regarding the prenatal origins of prostate diseases. The evidence shows that early prostate developmental processes are similar to the program controlling prostate cancer installation.[2] These events share similar gene expression programs, such as the acid phosphatase pathway, Wnt pathway, besides others associated with angiogenesis, apoptosis, migration, and cell proliferation.[2]

These studies have demonstrated that embryonic gene expression, sensitive to androgens, is activated during the processes involved in the initiation and progression of prostate cancer. Because prostate development is an event that depends on a finely regulated hormonal environment,[12,24,25] sensitive interferences may disrupt gene expression programs leading to irreversible changes in the pattern of prostate development and increasing the susceptibility to diseases with aging. Therefore, an understanding of the events that may interfere with prostate organogenesis may highlight the mechanisms involved during prostate disease.

This study identifies the early phases of prostate development as a determinant aspect for prostate gland morphogenesis. However,

as shown in previous studies by our group,[7,11,26] the female fetus was affected differently by testosterone exposure during the prenatal period, being masculinized and developing ectopic prostatic tissue around the vaginal wall. However, this study showed that although we did not observe any malformation of the male reproductive system, testosterone exposure during the prenatal phase associated with androgenic exposure during puberty seems to be associated with increased susceptibility to the development of benign diseases in these animals.

Moreover, evidence of a more proliferative prostate gland in animals exposed both prenatally and postnatally to testosterone indicates that the period of development of the prostate is determinant for the health of the gland during aging. We believe that the present study, although fundamentally based on morphological approaches, may contribute some additional information to a lacking area of research regarding the effects of prenatal androgenic imbalance and the consequences for the health of the prostate during aging periods.

A previous study[8] with male rats exposed to testosterone propionate during prenatal phase has not found important alterations regarding the prostate gland. However, there are some differences between the previous and the current study, such as the age of the animals, the experimental model, and the methodology. We worked with the tissues obtained from animals with 1-year-old. Indeed, there is a huge difference between the species employed in both works, especially regarding the prostate lesions. There are studies showing that the gerbils are rodents with a higher propensity for developing prostatic disorders.[15] Moreover, in our study we observed that only the group exposed with T during prenatal and pubertal phases developed adenomatous hyperplasia. However, despite these differences, new studies are necessary to clarify fundamental questions regarding the molecular biology of the effects of these androgen-induced changes during determinant periods of prostate development and its relation with the development of prostatic diseases in later stages.

Altogether, the evidence reinforces the potential that abnormal androgen exposure during prenatal phases associated with pubertal exposure may have effect on the prostate in terms of lesion development during aging. Although the hypothesis of the prenatal origins of prostate cancer has been debated lately as a strong candidate for the origin of prostate diseases,[2] conclusive studies are necessary in order to highlight the mechanisms underlying this complex field.

Some important factors such as inflammation seems to have an important role in BPH pathogenesis.[27,28] However, the underlying mechanisms related with the influence of inflammation on the prostate are not well understood. Although our study has shown the association of adenomatous hyperplasia with inflammation, it is uncertain if the disruption of the prostate was directly influenced by this inflammatory process. In a recent work published by our group, we found a similar condition in female models of gerbils. Female exposed to testosterone during prenatal and pubertal phases developed prostate glands affected with severe adenomatous hyperplasia associated with inflammation.[26] However, it is not clear to our group if the process of inflammation is the central cause of the prostatic lesions. More studies with different approaches are necessary to clarify these important issues.

Furthermore, studies focusing on the aromatization of testosterone in estradiol by aromatase (p450), or even testosterone conversion in dihydrotestosterone by 5α-reductase are approaches that need to be evaluated in future studies focusing on exogenous exposure to androgenic compounds, so that they may provide more insight into

how these substances are metabolized and act inside the organism in critical moments of the developmental period.

AUTHOR CONTRIBUTIONS

The work presented here was carried out as a collaboration. All of the authors (MFB, APSP, CRSC, LRFJr, RMG, PSLV, DRFJr, FCAS, and SRT) participated in the design, interpretation of the results, and review of the manuscript. MFB performed the experiments. MFB wrote the manuscript. DRFJr performed the kariometrical analysis. APSP, CRSC, LRFJr, RMG, PSLV, FCAS, and SRT equally contributed to the supervision of this work.

COMPETING INTERESTS

The authors declare neither conflict of interest nor competing financial interests for this work.

REFERENCES

1   Gardner WA. Hypothesis: the prenatal origins of prostate cancer. *Hum Pathol* 1995; 26: 1291–2.
2   Schaeffer EM, Marchionni L, Huang Z, Simons B, Blackman A, *et al*. Androgen-induced programs for prostate epithelial growth and invasion arise in embryogenesis and are reactivated in cancer. *Oncogene* 2008; 27: 7180–91.
3   Singh J, Handelsman DJ. Imprinting by neonatal sex steroids on the structure and function of the mature mouse prostate. *Biol Reprod* 1999; 61: 200–8.
4   Yarak S, Bagatin E, Hassun KM, Parada MO, Filho ST. Hyperandrogenism and skin: polycysic ovary syndrome and peripheral insulin resistance. *An Bras Dermatol* 2005; 80: 395–410.
5   Prins GS, Tang WL, Belmonte J, Ho SM. Perinatal exposure to oestradiol and bisphenol A alters the prostate epigenome and increases susceptibility to carcinogenesis. *Basic Clin Pharmacol Toxicol* 2008; 102: 134–8.
6   Timms BG, Howdeshell KL, Barton L, Bradley S, Richter C, *et al*. Estrogenic chemical in plastic and oral contraceptives disrupt development of the fetal mouse prostate and urethra. *Proc Natl Acad Sci U S A* 2005; 102: 7014–9.
7   Perez AP, Biancardi MF, Vilamaior PS, Góes RM, Santos FC, *et al*. Microscopic comparative study of the exposure effects of testosterone cypionate and ethinylestradiol during prenatal life on the prostatic tissue of adult gerbils. *Microsc Res Tech* 2012; 75: 1084–92.
8   Wolf CJ, Hotchkiss AK, Ostby JS, LeBlanc GA, Gray LE Jr. Effects of prenatal testosterone propionate on the sexual development of male and female rats: a dose-response study. *Toxicol Sci* 2002; 65: 71–86.
9   Hotchkiss AK, Furr J, Makynen EA, Ankley GT, Gray LE Jr. In utero exposure to the environmental androgen trenbolone masculinizes female Sprague-Dawley rats. *Toxicol Lett* 2007a; 174: 31–41.
10   Hotchkiss AK, Lambright CS, Ostby JS, Parks-Saldutti L, Vandenberg JG, *et al*. Prenatal testosterone exposure permanently masculinizes anogenital distance, nipple development, and reproductive tract morphology in female Sprague-Dawley rats. *Toxicol Sci* 2007b; 96: 335–45.
11   Biancardi MF, Perez AP, Góes RM, Santos FC, Vilamaior PS, *et al*. Prenatal testosterone exposure as a model for the study of endocrine-disrupting chemicals on the gerbil prostate. *Exp Biol Med* 2012; 237: 1298–309.
12   Timms BG. Prostate development: a historical perspective. *Differentiation* 2008; 76: 565–77.
13   Weibel ER. Principles and methods for the morphometric study of the lung and other organs. *Lab Invest* 1978; 12: 131–55.
14   Huttunen E, Romppanen T, Helminen HJ. A histoquantitative study on the effects of castration on the rat ventral prostate lobe. *J Anat* 1981; 3: 357–70.
15   Campos SG, Zanetoni C, Scarano WR, Vilamaior PS, Taboga SR. Age-related histopathological lesions in the Mongolian gerbil ventral prostate as a good model for studies of spontaneous hormone-related disorders. *Int J Exp Pathol* 2008; 89: 13–24.
16   Bostwick DG, Algaba F, Amin MB, Ayala A, Eble J, *et al*. Consensus statement on terminology: recommendation to use atypical adenomatous hyperplasia in place of adenosis of the prostate. *Am J Surg Pathol* 1994; 18: 1069–70.
17   Bostwick DG. Prostatic intraepithelial neoplasia and atypical adenomatous hyperplasia. *Cancer* 1996; 78: 330–6.
18   Zhang C, Montironi R, MacLennan GT, Lopez-Beltran A, Li Y, *et al*. Is atypical adenomatous hyperplasia of the prostate a precursor lesion? *Prostate* 2011; 71: 1746–51.
19   Santos FC, Leite RP, Custódio AM, Carvalho KP, Monteiro-Leal LH, *et al*. Testosterone stimulates growth and secretory activity of the female prostate in the adult gerbil (*Meriones unguiculatus*). *Biol Reprod* 2006; 75: 370–9.
20   Taboga SR, Santos AB, Gonzatti AG, Vidal BC, Mello ML. Nuclear phenotypes and morphometry of human secretory prostate cells: a comparative study of benign and malignant lesions in Brazilian patients. *Caryologia* (*Firenze*) 2003; 56: 313–20.
21   Ellem SJ, Risbridger GP. The dual, opposing roles of estrogen in the prostate. *Ann N Y Acad Sci* 2009; 1155: 174–86.
22   Grisanzio C, Signoretti S. p63 in prostate biology and pathology. *J Cell Biochem* 2008; 103: 1354–68.
23   De Marzo AM, Platz EA, Sutcliffe S, Xu J, Grönberg H, *et al*. Inflammation in prostate carcinogenesis. *Nature* 2007; 7: 256–69.
24   Thomson AA. Mesenchymal mechanisms in prostate organogenesis. *Differentiation* 2008; 76: 587–98.
25   Timms BG, Hofkamp L. Prostate development and growth in benign prostatic hyperplasia. *Differentiation* 2011; 82: 173–83.
26   Biancardi MF, Perez AP, Caires CR, Góes RM, Vilamaior PS, *et al*. Prenatal exposure to testosterone masculinises the female gerbil and promotes the development of lesions in the prostate (Skene's Gland). *Reprod Fertil Dev* 2014; doi: 10.1071/RD13387. [Epub ahead of print].
27   Corona G, Vignozzi L, Rastrelli G, Lotti F, Cipriani S, *et al*. Benign prostatic hyperplasia: a new metabolic disease of the aging male and its correlation with sexual dysfunctions. *Int J Endocrinol* 2014; 2014: 329456.
28   Vignozzi L, Rastrelli G, Corona G, Gacci M, Forti G, *et al*. Benign prostatic hyperplasia: a new metabolic disease? *J Endocrinol Invest* 2014; 37: 313–22.